arXiv:1711.01929v1 [physics.optics] 3 Nov 2017

Mean-field electron-vibrational theory of collective effects in photonic organic materials: bistability

Boris D. Fainberg
Faculty of Sciences, Holon Institute of Technology, 52 Golomb St., Holon 58102, Israel
Tel Aviv University, School of Chemistry, Tel Aviv 69978, Israel

2017/10/26

Abstract

Purely organic materials with negative and near-zero dielectric permittivity can be easily fabricated, and propagation of surface polaritons at the material/air interface was demonstrated. Here we develop a mean-field theory of light-induced optical properties of photonic organic materials taking the collective effects into account. The theory describes both a red shift of the resonance frequency of isolated molecules, according to the Clausius-Mossotti Lorentz-Lorentz mechanism, and the wide variations of their spectra related to the aggregation of molecules into J- or H-aggregates. We show that the experimental absorption spectra of H-aggregates may be correctly described only if one takes both mechanisms into account. The bistable response of organic materials in the condensed phase has been demonstrated using the electron-vibrational model. We show that using molecules with long-living triplet state T_1 near excited singlet state S_1, and fast intersystem crossing $S_1 \to T_1$ enables us to diminish CW light intensity needed for observing bistability below the damage threshold of thin organic films.

1 Introduction

Plasmonics and metamaterials provide great scope for concentrating and manipulating the electromagnetic field on the subwavelength scale to achieve dramatic enhancement of optical processes and to develop super-resolution imaging, optical cloaking etc.[1–4] However, metallic inclusions in metamaterials are sources of strong absorption loss. This hinders many applications of metamaterials and plasmonics and motivates to search for efficient solutions to the loss problem.[5] Highly doped semiconductors[5,6] and doped graphene[7–9] can in principle solve the loss problem. However, the plasmonic frequency in these materials is an order of magnitude lower than that in metals making former most useful at mid-IR and THz regions. In this relation the question arises whether metal-free metamaterials and plasmonic systems, which do not suffer from excessive damping loss, can be realized in the visible range? With no doubts, inexpensive materials with such advanced properties can impact whole technological fields of nanoplasmonics and metamaterials.

Recently Noginov et al. demonstrated that purely organic materials characterized by low losses with negative, near-zero, and smaller than unity dielectric permittivities can be easily fabricated.[10] Specifically, the substantially strong negative dielectric permittivity demonstrated in zinc tetraphenylporphyrin (ZnTPP), suggests that this dye compound can function as a plasmonic material. The experimental demonstration of a surface polariton propagating at the ZnTPP/air interface has been realized.[10]

In addition, Gentile et al.[11] showed that polymer films doped with J-aggregated (TDBC) molecules might exhibit a negative real permittivity in the vicinity of the exciton resonance. Thin films of

such material may support surface exciton-polariton modes, in much the same way that thin metal films support surface plasmon-polariton modes. Furthermore, they used the material parameters derived from experiment to demonstrate that nanostructured excitonic materials may support localized surface exciton-polariton modes.

Moreover, near-zero dielectric permittivity of the organic host medium results in dramatic enhancement of intersite dipolar energy-transfer interaction in the quantum dot wire that influences on electron transport through nanojunctions.[12] Such interactions can compensate Coulomb repulsions in the wire for particular conditions.[12–14] And even the dramatic laser-induced change of the dielectric permittivity of dyes may be realized[12,15] that can enable us to control their "plasmonic" properties.

Both approaches[10] and[11] were explained in simple terms of the Lorentz model for linear spectra of dielectric permittivities of thin film dyes. However, the experiments with strong laser pulses[15] will challenge theory. The point is that the Lorentz model based on a mean-field theory is described by essentially nonlinear equations for strong laser excitation. Their general solution is not a simple problem. In addition, such nonlinear equations can predict switching waves,[16] bistability etc.

Here we develop an electron-vibrational theory of light-induced optical properties of photonic organic materials taking the collective effects into account. Our consideration is based on the model of the interaction of strong shaped laser pulse with organic molecules, Refs.,[17–19] extended to the dipole-dipole intermolecular interactions in the condensed matter. These latters are taken into account using a mean-field theory that resulted in two options: one mother - two daughters. The first option correctly describes the behaviour of the first moment of molecular spectra in condensed matter, and specifically, the red shift, according to the Clausius-Mossotti Lorentz-Lorentz (CMLL) mechanism.[20] The second option is related to the dramatic modification of molecular spectra in condensed matter due to aggregation of molecules into J- or H-aggregates. Among other things we demonstrate the bistable response of organic materials in the condensed phase using the electron-vibrational model. It is worthy to note that a bistable behavior of molecular J-aggregates in the context of purely electronic theory was demonstrated in Refs.[21,22] At the same time, as shown below, the vibrations can give rather important contribution to broadening aggregate spectra that may be crucial, in spite of strong narrowing the J-aggregate spectra with respect to the spectra of monomer molecules. We also consider the problem of diminishing light intensity necessary for bistablity below the damage threshold of thin organic films.

The paper is organized as follows. We start with the derivation of equations taking dipole-dipole intermolecular interactions in condensed matter into account. In Sections 3 and 4 we consider two options of the mean-field theory resulting to the self-energy depending and not depending, respectively, on effective vibrational coordinate. Then we describe the absorption of H-aggregates, Section 5, where we show that only taking both options of our mean-field theory into account can explain the experimental results. In Section 6 we consider bistability, and in Section 7, we briefly conclude.

2 Derivation of equations for dipole-dipole intermolecular interactions in condensed matter

In this section we shall extend our picture of "moving" potentials of Ref.[17] to a condensed matter. In this picture we considered a molecule with two electronic states $n = 1$ (ground) and 2 (excited) in a solvent described by the Hamiltonian

$$H_0 = \sum_{n=1}^{2} |n\rangle \left[E_n + W_n(\mathbf{Q})\right] \langle n| \qquad (1)$$

where $E_2 > E_1, E_n$ is the energy of state $n, W_n(\mathbf{Q})$ is the adiabatic Hamiltonian of reservoir R (the vibrational subsystems of a molecule and a solvent interacting with the two-level electron system under consideration in state n). The molecule is affected by electromagnetic field $\mathbf{E}(t)$

$$\mathbf{E}(t) = \frac{1}{2}\mathbf{e}\mathcal{E}(t)\exp(-i\omega t) + \text{c.c.} \quad (2)$$

the frequency of which is close to that of the transition $1 \to 2$. Here $\mathcal{E}(t)$ describes the change of the pulse amplitude in time, $\mathbf{e}$ is unit polarization vector.

One can describe the influence of the vibrational subsystems of a molecule and a solvent on the electronic transition within the range of definite vibronic transition related to a high frequency optically active (OA) vibration as a modulation of this transition by low frequency (LF) OA vibrations $\{\omega_s\}$.[23] In accordance with the Franck-Condon principle, an optical electronic transition takes place at a fixed nuclear configuration. Therefore, the quantity $u_1(\mathbf{Q}) = W_2(\mathbf{Q}) - W_1(\mathbf{Q}) - \langle W_2(\mathbf{Q}) - W_1(\mathbf{Q})\rangle_1$ representing electron-vibration coupling is the disturbance of nuclear motion under electronic transition where $\langle\rangle_n$ stands for the trace operation over the reservoir variables in the electronic state n. Electronic transition relaxation stimulated by LFOA vibrations is described by the correlation function $K(t) = \langle\alpha(0)\alpha(t)\rangle$ of the corresponding vibrational disturbance with characteristic attenuation time τ_s[24–26] where $\alpha \equiv -u_1/\hbar$. The analytic solution of the problem under consideration has been obtained due to the presence of a small parameter. For broad vibronic spectra satisfying the "slow modulation" limit, we have $\sigma_{2s}\tau_s^2 \gg 1$ where $\sigma_{2s} = K(0)$ is the LFOA vibration contribution to a second central moment of an absorption spectrum, the half bandwidth of which is related to σ_{2s} as $\Delta\omega_{abs} = 2\sqrt{2\sigma_{2s}\ln 2}$. According to Refs.,[25,26] the following times are characteristic for the time evolution of the system under consideration: $\sigma_{2s}^{-1/2} < T' << \tau_s$, where $\sigma_{2s}^{-1/2}$ and $T' = (\tau_s/\sigma_{2s})^{1/3}$ are the times of reversible and irreversible dephasing of the electronic transition, respectively. The characteristic frequency range of changing the optical transition probability can be evaluated as the inverse T', i.e. $(T')^{-1}$. Thus, one can consider T' as a time of the optical electronic transition. Therefore, the inequality $\tau_s \gg T'$ implies that the optical transition is instantaneous where relation $T'/\tau_s << 1$ plays the role of a small parameter.

This made it possible to describe vibrationally nonequilibrium populations in electronic states 1 and 2 by balance equations for the intense pulse excitation (pulse duration $t_p > T'$) and solve the problem.[17,27]

Let us include now the dipole-dipole intermolecular interactions in the condensed matter that are described by Hamiltonian[24,28] $H_{int} = \hbar \sum_{m\neq n} J_{mn} b_m^\dagger b_n$. Then Eq.(6) of Ref.[17] describing vibrationally nonequilibrium populations in electronic states $j = 1, 2$ for the exponential correlation function $K(t)/K(0) \equiv S(t) = \exp(-|t|/\tau_s)$ can be written as

$$\begin{aligned}\frac{\partial}{\partial t}\rho_{jj}(\alpha,t) &= -i\hbar^{-1}[H_0(\alpha,t) + H_{int} - \mathbf{D}\cdot\mathbf{E}(t), \rho(\alpha,t)]_{jj} \\ &\quad + L_{jj}\rho_{jj}(\alpha,t) \end{aligned} \quad (3)$$

where $j = 1, 2$; and the operator L_{jj} is determined by the equation:

$$L_{jj} = \tau_s^{-1}\left[1 + (\alpha - \delta_{j2}\omega_{st})\frac{\partial}{\partial(\alpha - \delta_{j2}\omega_{st})} + \sigma_{2s}\frac{\partial^2}{\partial(\alpha - \delta_{j2}\omega_{st})^2}\right], \quad (4)$$

describes the diffusion with respect to the coordinate α in the corresponding effective parabolic potential $U_j(\alpha)$, δ_{ij} is the Kronecker delta, $\omega_{st} = \beta\hbar\sigma_{2s}$ is the Stokes shift of the equilibrium absorption and luminescence spectra, $\beta = 1/k_BT$. In the absence of the dipole-dipole intermolecular interactions in the condensed matter, H_{int}, Eq.(3) is reduced to Eq.(11) of Ref.[17] The partial density matrix of the system $\rho_{jj}(\alpha,t)$ describes the system distribution in states 1 and 2 with a given value of α at time t. The complete density matrix averaged over the stochastic process which modulates the system energy levels, is obtained by integration of $\rho_{ij}(\alpha,t)$ over α, $\langle\rho\rangle_{ij}(t) = \int \rho_{ij}(\alpha,t)\,d\alpha$, where quantities $\langle\rho\rangle_{jj}(t)$ are the normalized populations of the corresponding electronic states: $\langle\rho\rangle_{jj}(t) \equiv n_j$, $n_1 + n_2 = 1$. Knowing $\rho_{jj}(\alpha,t)$, one can calculate the positive frequency component of the polarization $\mathbf{P}^{(+)}(t) = N\mathbf{D}_{12}\langle\rho\rangle_{21}(t)$, and the susceptibility $\chi(\Omega,t)$[17] that enables us to obtain the dielectric function ε due to relation $\varepsilon(\Omega,t) = 1 + 4\pi\chi(\Omega,t)$. Here N is the density of molecules. It is worthy to note that magnitude $\varepsilon(\Omega,t)$ does make sense, since it changes in time slowly with respect to dephasing. In other words, $\varepsilon(\Omega,t)$ changes in time slowly with respect to reciprocal characteristic frequency domain of changing $\varepsilon(\Omega)$.

Consider the contribution of Hamiltonian $\hat{H}_{int}$ to the change of $\rho_{ij}(\alpha,t)$ in time. In other words, we shall generalize Eq.(11) of Ref.[17] to the dipole-dipole intermolecular interactions in the condensed matter. Using the Heisenberg equations of motion, one obtains that $\hat{H}_{int}$ gives the following contribution to the change of the expectation value of excitonic operator b_k in time

$$\begin{aligned}\frac{d}{dt}\langle b_k\rangle &\sim \frac{i}{\hbar}\langle[\hat{H}_{int},b_k]\rangle \equiv \frac{i}{\hbar}Tr([\hat{H}_{int},b_k]\rho)\\ &= -i\sum_{n\neq k}J_{kn}\langle(\hat{n}_{k1}-\hat{n}_{k2})b_n\rangle \qquad (5)\end{aligned}$$

where $\hat{n}_{k1}=b_kb_k^{\dagger}$, and $\hat{n}_{k2}=b_k^{\dagger}b_k$ is the exciton population operator. Considering an assembly of identical molecules, one can write $\langle b_k\rangle=\rho_{21}(\alpha,t)$[29] if averaging in Eq.(5) is carried out using density matrix $\rho(\alpha,t)$. Consider the expectation value $\langle(\hat{n}_{k1}-\hat{n}_{k21})b_n\rangle=Tr[(\hat{n}_{k1}-\hat{n}_{k2})b_n\rho(\alpha_k,\alpha_n,t)]$ for $n\neq k$ where α_m is the effective vibrational coordinate of a molecule m $(m=k,n)$. Due to fast dephasing (see above), it makes sense to neglect all correlations among different molecules,[24] and set $\langle(\hat{n}_{k1}-\hat{n}_{k2})b_n\rangle=\langle\hat{n}_{k1}-\hat{n}_{k2}\rangle\langle b_n\rangle$ and correspondingly $\rho(\alpha_k,\alpha_n,t)\simeq\rho(\alpha_k,t)\rho(\alpha_n,t)$, i.e. density matrix $\rho(\alpha_k,\alpha_n,t)$ is factorized. Here from dimension consideration one expectation value should be calculated using density matrix $\rho(\alpha,t)$, and another one - using $\langle\rho\rangle(t)=\int\rho(\alpha,t)\,d\alpha$. Since we sum with respect to n, it would appear reasonable to integrate with respect to α_n. However, this issue is not so simple. The point is that in addition to intramolecular vibrations, there is a contribution of low-frequency intermolecular and solvent coordinates into effective coordinate α. Because of this, partitioning the vibrations into α_k and α_n groups is ambiguous, and the mean-field approximation gives two options

$$p\langle b\rangle\langle\hat{n}_1-\hat{n}_2\rangle=\begin{pmatrix}p\rho_{21}(\alpha,t)\Delta n\\ p\langle\rho_{21}\rangle(t)\Delta'(\alpha,t)\end{pmatrix} \qquad (6)$$

where $\Delta'(\alpha,t)=\rho_{11}(\alpha,t)-\rho_{22}(\alpha,t)$, $p\equiv-\sum_{n\neq k}J_{kn}$, $\Delta n\equiv n_1-n_2$. Below we shall discuss which option better corresponds to a specific experimental situation. Consideration based on nonequilibrium Green functions (GF) shows that the terms $p\rho_{21}(\alpha,t)$ and $p\langle\rho_{21}\rangle(t)$ on the right-hand-side of Eq.(6) represent the self-energy, $\Sigma_{21}(t)$, and the terms Δn and $\Delta'(\alpha,t)$ - the difference of the "lesser" GFs for equal time arguments, $G_{11}^{<}(t,t)-G_{22}^{<}(t,t)$, that are the density matrix, i.e. $p\langle b\rangle\langle\hat{n}_1-\hat{n}_2\rangle=\Sigma_{21}(t)[G_{11}^{<}(t,t)-G_{22}^{<}(t,t)]$, respectively. In other words, for the first line on the right-hand-side of Eq.(6), the self-energy depends on α and the "lesser" GFs $G_{11}^{<}(t,t)-G_{22}^{<}(t,t)$ do not. In contrast, for the second line on the right-hand-side of Eq.(6), the self-energy does not depend on α and the "lesser" GFs $G_{11}^{<}(\alpha;t,t)-G_{22}^{<}(\alpha;t,t)$ do depend. This yields $\partial\rho_{21}(\alpha,t)/\partial t\sim i\Sigma_{21}(t)[G_{11}^{<}(t,t)-G_{22}^{<}(t,t)]$. Adding term "$i\Sigma_{21}(t)[G_{11}^{<}(t,t)-G_{22}^{<}(t,t)]$" to the right-hand side of Eq.(9) of Ref.[17]

$$\begin{aligned}&\frac{\partial}{\partial t}\tilde{\rho}_{21}(\alpha,t)+i(\omega_{21}-\omega-\alpha)\tilde{\rho}_{21}(\alpha,t)\\ \approx\ &\frac{i}{2\hbar}\mathbf{D}_{21}\cdot\mathbf{E}(t)\Delta'(\alpha,t)+i\tilde{\Sigma}_{21}(t)[G_{11}^{<}(t,t)\\ &-G_{22}^{<}(t,t)] \qquad (7)\end{aligned}$$

where $\tilde{\rho}_{21}=\rho_{21}\exp(i\omega t)$, $\tilde{\Sigma}_{21}=\Sigma_{21}\exp(i\omega t)$, and using the procedure described there, we get the extensions of Eq.(11) of Ref.[17] to the dipole-dipole intermolecular interactions in the condensed matter.

3 Self-energy depending on effective vibrational coordinate α

Consider first the case of self-energy depending on effective vibrational coordinate α (the first line on the right-hand-side of Eq.(6)) when the main contribution to α is due to low-frequency intermolecular vibrations and solvent coordinates. Then we arrive to equation

$$\begin{aligned}\frac{\partial\rho_{jj}(\alpha,t)}{\partial t} &= L_{jj}\rho_{jj}(\alpha,t)+\frac{(-1)^j\pi}{2}\Delta'(\alpha,t)|\Omega_R(t)|^2\times\\ &\quad\times\delta[\omega_{21}-p\Delta n-\omega-\alpha] \qquad (8)\end{aligned}$$

where ω_{21} is the frequency of Franck-Condon transition $1\rightarrow2$, $\Omega_R(t)=(\mathbf{D}_{12}\cdot\mathbf{e})\mathcal{E}(t)/\hbar$ is the Rabi

frequency, $\mathbf{D}_{12}$ is the electronic matrix element of the dipole moment operator.

As one can see from Eq.(8), self-energy $\Sigma_{21}(t) = p\rho_{21}(\alpha,t)$ results in the frequency shift of spectra "$-p\Delta n$" without changing the line shapes.[12] One can show that this approach correctly describes the change of the first moment of optical spectra in the condensed matter. Calculations of p for isotropic medium give $p = \frac{4\pi}{3\hbar}|D_{12}|^2 N > 0$ [12,24,30] that corresponds to a red shift, according to the Clausius-Mossotti Lorentz-Lorentz (CMLL) mechanism.[20]

Integration of Eq.(8) is achieved by the Green's function[27]

$$G_{jj}(\alpha,t;\alpha',t') = \frac{1}{\sqrt{2\pi\sigma(t-t')}}\exp\{-[(\alpha-\delta_{j2}\omega_{st}) - (\alpha'-\delta_{j2}\omega_{st})S(t-t')]^2/(2\sigma(t-t'))\} \quad (9)$$

where $\sigma(t-t') = \sigma_{2s}\left[1-S^2(t-t')\right]$, for the initial condition,

$$\rho_{jj}^{(0)}(\alpha) \equiv \rho_{jj}(\alpha,t=0) = \delta_{j1}(2\pi\sigma_{2s})^{-1/2}\exp(-\frac{\alpha^2}{2\sigma_{2s}}) \quad (10)$$

We obtain

$$\begin{aligned}\rho_{jj}(\alpha,t) &= \rho_{jj}^{(0)}(\alpha) + (-1)^j\frac{\pi}{2} \\ &\times\int_0^t dt'|\Omega_R(t')|^2\Delta'(\omega_{21}-p\Delta n-\omega,t') \\ &\times G_{jj}(\alpha,t;\omega_{21}-p\Delta n-\omega,t') \quad (11)\end{aligned}$$

where $\Delta'(\omega_{21}-p\Delta n-\omega,t')$ satisfies nonlinear integral equations that can be easily obtained from Eq.(11). Integrating both sides of Eq.(11) with respect to α and bearing in mind that $\int_{-\infty}^{\infty} G_{jj}(\alpha,t;\omega_{21}-\omega(t'),t')\,d\alpha = 1$, we get

$$\frac{dn_j}{dt} = (-1)^j\frac{\pi}{2}|\Omega_R(t)|^2\Delta'(\omega_{21}-p\Delta n-\omega,t) \quad (12)$$

3.1 Fast vibrational relaxation

Let us consider the particular case of fast vibrational relaxation when one can put the normalized correlation function $S(t-t') \equiv K(t-t')/K(0)$ equal to zero. Physically it means that the equilibrium distributions into the electronic states have had time to be set during changing the pulse parameters. Bearing in mind that for fast vibronic relaxation

$$\begin{aligned}\Delta'(\alpha,t) &= \frac{n_1(t)}{(2\pi\sigma_{2s})^{1/2}}\exp(-\frac{\alpha^2}{2\sigma_{2s}}) - \\ &-\frac{n_2(t)}{(2\pi\sigma_{2s})^{1/2}}\exp[-\frac{(\alpha-\omega_{st})^2}{2\sigma_{2s}}] \quad (13)\end{aligned}$$

substituting the last equation into Eq.(12) and using Eq.(19), one gets

$$\begin{aligned}\frac{dn_j}{dt} &= (-1)^j\sigma_a(\omega_{21})\tilde{J}(t)\,\mathrm{Re}[n_1\bar{W}_a(\omega+p\Delta n) - \\ &-n_2\bar{W}_f(\omega+p\Delta n)] - (-1)^j\frac{n_2}{T_1} \quad (14)\end{aligned}$$

where $n_1+n_2=1$, σ_a is the cross section at the maximum of the absorption band, $\tilde{J}(t)$ is the power density of exciting radiation, $\bar{W}_{a(f)}(\omega) = W_{a(f)}(\omega)/F_{a,\max}$, and we added term "$(-1)^j n_2/T_1$" taking the lifetime T_1 of the excited state into account. Here "$-iW_{a(f)}(\omega)$" is the line-shape function of a monomer molecule for the absorption (fluorescence) for fast vibronic relaxation, and

$$\begin{aligned}&\int_{-\infty}^{\infty} d\alpha\Delta'(\alpha,t)\,\zeta(\omega-\omega_{21}+\alpha)/\pi \\ &= -i[n_1(t)W_a(\omega) - n_2(t)W_f(\omega)] \quad (15)\end{aligned}$$

where $\zeta(\omega-\omega_{21}+\alpha) = \frac{P}{\omega-\omega_{21}+\alpha} - i\pi\delta(\omega-\omega_{21}+\alpha)$, P is the symbol of the principal value.

The imaginary part of "$-iW_{a(f)}(\omega)$" with sign minus, $-\mathrm{Im}[-iW_{a(f)}(\omega)] = \mathrm{Re}\,W_{a(f)}(\omega) \equiv F_{a(f)}(\omega)$, describes the absorption (fluorescence) lineshapes of a monomer molecule, and the real part, $\mathrm{Re}[-iW_{a(f)}(\omega)] = \mathrm{Im}\,W_{a(f)}(\omega)$, describes the corresponding refraction spectra.

For the "slow modulation" limit considered in this section,

$$W_{a(f)}(\omega) = \sqrt{\frac{1}{2\pi\sigma_{2s}}}w(\frac{\omega-\omega_{21}+\delta_{a(f),f}\omega_{st}}{\sqrt{2\sigma_{2s}}}) \quad (16)$$

where $w(z) = \exp(-z^2)[1 + i\,\mathrm{erf}\, i(z)]$ is the probability integral of a complex argument,[31] and

$$F_{a(f)}(\omega) = \sqrt{\frac{1}{2\pi\sigma_{2s}}}\exp[-\frac{\left(\omega_{21} - \omega - \delta_{a(f),f}\omega_{st}\right)^2}{2\sigma_{2s}}] \tag{17}$$

4 Population difference ("lesser" GFs) depending on effective vibrational coordinate α

Consider now the case when the population difference depends on effective vibrational coordinate α (the second line on the right-hand-side of Eq.(6); the main contribution to α is due to intramolecular vibrations). Then we arrive to equation

$$\begin{aligned}\frac{\partial\rho_{jj}(\alpha,t)}{\partial t} &= L_{jj}\rho_{jj}(\alpha,t) + \frac{(-1)^j\pi}{2}\Delta'(\alpha,t) \\ &\times\delta(\omega_{21} - \omega - \alpha)\,|\Omega_{eff}(t)|^2 \end{aligned} \tag{18}$$

where $\Omega_{eff}(t) = \Omega_R(t) + 2p\langle\rho_{21}\rangle(t) = \Omega_R(t) + 2\Sigma_{21}(t)$ is the effective Rabi frequency that can be written as

$$\Omega_{eff}(t) = \frac{\Omega_R(t)}{1 + p\int d\alpha\Delta'(\alpha,t)\,\zeta(\omega - \omega_{21} + \alpha)}, \tag{19}$$

Here $\int d\alpha\Delta'(\alpha,t)\,\zeta(\omega - \omega_{21} + \alpha)/\pi$ is the line-shape function that is reduced to that of a monomer molecule in the absense of the dipole-dipole interactions for the equilibrium value of $\Delta'(\alpha,t)$.

One can see that in contrast to the self-energy depending on effective vibrational coordinate α, Section 3, here the self-energy $\Sigma_{21}(t) = p\langle\rho_{21}\rangle(t)$ (the second line on the right-hand-side of Eq.(6)) results in the change of both the frequency shift of spectra and their lineshapes. In that case considering the dense collection of molecules under the action of one more (weak) field

$$\tilde{\mathbf{E}}(t) = \frac{1}{2}\mathbf{e}\tilde{\mathcal{E}}(t)\exp(-i\Omega t) + \text{c.c.},$$

one gets for the positive frequency component of the polarization $\mathbf{P}^+ = N\mathbf{D}_{12}\langle\rho_{21}\rangle(t)$

$$\mathbf{P}^+(\Omega,t) = \frac{-N\mathbf{D}_{12}(\mathbf{D}_{21}\cdot\mathbf{e})\tilde{\mathcal{E}}(t)/(6\hbar)}{[\int d\alpha\Delta'(\alpha,t)\,\zeta(\Omega - \omega_{21} + \alpha)]^{-1} + p}, \tag{20}$$

for the susceptibility

$$\chi(\Omega,t) = -\frac{N|D_{12}|^2}{3\hbar}\frac{\int d\alpha\Delta'(\alpha,t)\,\zeta(\Omega - \omega_{21} + \alpha)}{1 + p\int d\alpha\Delta'(\alpha,t)\,\zeta(\Omega - \omega_{21} + \alpha)} \tag{21}$$

and the dielectric function

$$\begin{aligned}\varepsilon(\Omega,t) &= 1 - 4\pi\frac{N|D_{12}|^2}{3\hbar} \\ &\times\frac{\int d\alpha\Delta'(\alpha,t)\,\zeta(\Omega - \omega_{21} + \alpha)}{1 + p\int d\alpha\Delta'(\alpha,t)\,\zeta(\Omega - \omega_{21} + \alpha)}\end{aligned} \tag{22}$$

It is worthy to note that the "slow modulation" limit underlying Eq.(18) can break down in the case of the formation of J-aggregates possessing rather narrow spectra. In such a case one should use more general theory that is not based on the approximation of broad vibronic spectra. Below we shall consider the case of fast vibrational relaxation that is not limited by the "slow modulation".

4.1 Line-shape in the fast vibrational relaxation limit

We shall see below that the approximation based on the self-energy integrated on the effective vibrational coordinate (the second line on the right-hand-side of Eq.(6)) correctly describe the exciton spectra. In this relation, the fast vibrational relaxation limit for the case under consideration should be used with caution. The point is that the equilibrium state under study is rather the equilibrium state of the collective system (molecules coupled by the dipole-dipole interaction) than that of separate molecules. However, the exciton wave function in the ground state is the product of the wave functions of monomers[28] (no intermolecular interactions). Because of this, Eq.(18) for the absorption of weak radiation and $j = 1$ can be written as

$$\frac{\partial \rho_{11}(\alpha,t)}{\partial t} = L_{11}\rho_{11}(\alpha,t) - \frac{\pi}{2}\Delta'^{(0)}(\alpha,t) \times\delta(\omega_{21}-\omega-\alpha)\,|\Omega^{(0)}_{eff}(t)|^2 \quad (23)$$

where

$$\Omega^{(0)}_{eff}(t) = \frac{\Omega_R(t)}{1+p\int d\alpha\Delta'^{(0)}(\alpha)\,\zeta(\omega-\omega_{21}+\alpha)}, \quad (24)$$

$\Delta'^{(0)}(\alpha) = \rho^{(0)}_{11}(\alpha) = (2\pi\sigma_{2s})^{-1/2}\exp[-\alpha^2/(2\sigma_{2s})]$ is the equilibrium value of $\Delta'(\alpha,t)$ corresponding to the equilibrium value for a monomer in the ground state, and we retained only terms that are proportional to $|\Omega_R(t)|^2$ on the right-hand side of Eq.(23). The next procedure is similar to that used for obtaining Eq.(14) (see above). Integrating Eq.(23), using Green function, Eq.(9), we obtain an integral equation that is similar to Eq.(11). Then integrating both sides of the obtained integral equation with respect to α, and bearing in mind Eq.(15), we get

$$\frac{dn_1}{dt} = -\sigma_a(\omega_{21})\tilde{J}(t)\,\mathrm{Re}\,\frac{\bar{W}_a(\omega)}{1-ip\pi W_a(\omega)} + \frac{n_2}{T_1} \quad (25)$$

where the term $\mathrm{Re}\{\bar{W}_a(\omega)/[1-ip\pi W_a(\omega)]\}$ describes the absorption spectrum of molecules susceptible to the dipole-dipole intermolecular interactions expressed through their monomer spectra W_a. This term agrees with the coherent exciton scattering (CES) approximation.[32–34] The latter is well suited to describe absorption spectra of both J- and H-aggregates using their monomer spectra and the intermolecular interaction strength that is a fitting parameter.

It is worthy to note that the term $1/[1-ip\pi W_a(\omega)]$ on the right-hand side of Eq.(25) amounts to the Pade approximant $[0/1]$[35] that is the sum of diagrams of a certain type.[36] Indeed, the term under discussion is the sum of the infinite geometrical series

$$\frac{1}{1-ip\pi W_a(\omega)} = \sum_{m=0}^{\infty} p^m[i\pi W_a(\omega)]^m \quad (26)$$

where the right-hand side of Eq.(26) multiplied by $W_a(\omega)$ may be considered as a Born series with the interaction parameter p.

4.1.1 Description of the absorption of J-aggregates

Applying expression $\mathrm{Re}\{\bar{W}_a(\omega)/[1-ip\pi W_a(\omega)]\}$ to the description of the absorption of J-aggregates, one should take into account that the Gaussian shape of the monomer absorption spectrum obtained in the "slow modulation" limit is correct only near the absorption maximum. The wings decline much slower as $(\omega_{21}-\omega)^{-4}$.[37] At the same time, the expression under discussion has a pole, giving strong absorption, when $1/(p\pi) = -\,\mathrm{Im}\,W_a(\omega)$. If parameter of the dipole-dipole intermolecular interaction p is rather large, the pole may be at a large distance from the absorption band maximum where the "slow modulation" limit breaks down. This means one should use exact expression for the monomer spectrum W_a that is not limited by the "slow modulation" approximation, and properly describe both the central spectrum region and its wings. The exact calculation of the vibrationally equilibrium monomer spectrum for the Gaussian-Markovian modulation with the exponential correlation function $S(t) = \exp(-|t|/\tau_s)$ gives[37,38] (see Appendix)

$$W_a(\omega) = \frac{\tau_s}{\pi}\frac{\Phi(1,1+x_a;\sigma_{2s}\tau_s^2)}{x_a} \quad (27)$$

where $x_a = \tau_s/(2T_1) + \sigma_{2s}\tau_s^2 + i\tau_s(\omega_{21}-\omega)$, $\Phi(1,1+x_a;\sigma_{2s}\tau_s^2)$ is a confluent hypergeometric function.[31]

Figs. 1, 2 and 3 show the calculation results of the absorption spectra of J-aggregates according to the expression $\mathrm{Re}\{W_a(\omega)/[1-ip\pi W_a(\omega)]\}$ on the right-hand side of Eq.(25) and Eq.(27), and their comparison with the monomer spectra $\mathrm{Re}\,W_a(\omega)$. The spectra of Fig.1 correspond to a dense collection of molecules ($N = 10^{21}cm^{-3}$, Ref.[10]) with parameters close to those of molecule LD690:[17] $\sqrt{\sigma_{2s}} = 546$ cm^{-1}, $\tau_s = 10^{-13}s$, $D_{12} = 10^{-17}$ CGSE that gives $\omega_{st} = 1420$ cm^{-1}, $p = 2107$ cm^{-1}. We put $T_1 = 10^{-9}s$.

One can see that in spite of strong narrowing the J-aggregate spectra with respect to those of monomers, the vibrations still give rather important contribution to broadening the J-aggregate spectra that may be crucial. Indeed, the half bandwidth of the J-aggregate absorption spectrum is about $3\cdot10^{12}$ rad/s

Figure 1: Absorption spectra (in terms of τ_s/π) of the J-aggregate (solid line) and the corresponding monomer (dashed line) in the case of slow modulation ($\sqrt{\sigma_{2s}}\tau_s = 10.9 >> 1$). Dimensionless parameter is $\Delta = \tau_s(\omega_{21} - \omega)$.

that may far exceed the lifetime contribution. So, disregarding vibrations in the description of the J-aggregate spectra may be incorrect. Moreover, above parameters for molecule LD690 in methanol were obtained using only LFOA vibrations $\{\omega_s\}$ for the simulation of its spectra. If one in addition uses also high frequency OA intramolecular vibrations (like C-C $\sim$ 1400 cm^{-1}) for the simulation (see below), then the second central moment σ_{2s} should be related rather to a vibronic transition with respect to the high frequency OA vibration than to the whole spectrum, i.e. the value of σ_{2s} diminishes. Fig.2 shows absorption spectra of the J-aggregate and the corresponding monomer when parameter $\sqrt{\sigma_{2s}}\tau_s = 3.16$ is smaller than that for Fig.1. One can see lesser narrowing the J-aggregate spectrum with respect to that of a monomer. In contrast, the J-aggregate absorption spectrum calculated using the monomer spectrum W_a, Eq.(16), and, as a consequence, the Gaussian absorption spectrum, Eq.(17), is extremely narrow (see also[34]).

For fast modulation when $\sigma_{2s}\tau_s^2 << 1$, the aggregate spectrum only shifts with respect to the monomer one almost without changing its shape (Fig.3). Indeed, $\Phi(1, 1 + x_{a(f)}; \sigma_{2s}\tau_s^2) \approx 1$ for

Figure 2: Absorption spectra (in terms of τ_s/π) of the J-aggregate (solid line) and the corresponding monomer (dashed line) for $\sqrt{\sigma_{2s}}\tau_s = 3.16$ and $p\tau_s = 5$.

$\sigma_{2s}\tau_s^2 << 1$. In that case $W_a(\omega) \approx (\tau_s/\pi)/x_a$, and the term $\mathrm{Re}\{\bar{W}_a(\omega)/[1 - ip\pi W_a(\omega)]\}$ on the right-hand side of Eq.(25) becomes

$$\begin{aligned} \mathrm{Re}\,\frac{W_a(\omega)}{1 - ip\pi W_a(\omega)} &\approx \frac{1}{\pi}\,\mathrm{Re}\,\frac{1}{\frac{1}{2T_1} + \sigma_{2s}\tau_s + i(\omega_{21} - \omega - p)} \\ &= W_a(\omega + p) \end{aligned} \tag{28}$$

In other words, if the monomer spectrum has Lorentzian shape, the aggregate spectrum is simply shifted monomer spectrum. In that case both the approach based on the self-energy depending on the effective vibrational coordinate, and the approach based on the population difference ("lesser" GFs) depending on the effective vibrational coordinate give the same absorption spectrum of molecules susceptible to the dipole-dipole intermolecular interactions.

5 Description of the absorption of H-aggregates

Applying expression $\mathrm{Re}\{W_a(\omega)/[1 - ip\pi W_a(\omega)]\}$ (see Section4.1) to the description of the absorption of H-aggregates, one should take into account also high frequency OA intramolecular vibrations,[33] in addition to the LFOA vibrations $\{\omega_s\}$ under consideration in our paper. The general form of Eq.(25) enables us to do this. We will consider one normal high frequency intramolecular oscillator of frequency ω_0 whose equilibrium position is shifted under electronic transition. Its characteristic function $f_{\alpha M}(t)$ is determined by the following expression:[18,39]

$$\begin{aligned} f_{\alpha M}(t) &= \exp(-S_0 \coth\theta_0) \sum_{k=-\infty}^{\infty} I_k(S_0/\sinh\theta_0) \\ &\quad \times \exp[k(\theta_0 + i\omega_0 t)] \end{aligned} \tag{29}$$

where S_0 is the dimensionless parameter of the shift, $\theta_0 = \hbar\omega_0/(2k_BT)$, $I_n(x)$ is the modified Bessel func-

Figure 3: Absorption spectra (in terms of τ_s/π) of the J-aggregate (solid line) and the corresponding monomer (dashed line) in the case of fast modulation ($\sqrt{\sigma_{2s}}\tau_s = 0.1 << 1$) for $p\tau_s = 0.3$.

tion of first kind.[31] Then $W_a(\omega)$ can be written as

$$\begin{aligned} W_a(\omega) &= \frac{1}{\pi}\int_0^\infty f^*_{\alpha M}(t)\exp[i(\omega-\omega_{21})t+g_s(t)]dt \\ &= \sum_{k=-\infty}^{\infty}\frac{\exp(-S_0\coth\theta_0+k\theta_0)}{\pi}I_k(\frac{S_0}{\sinh\theta_0}) \\ &\quad\times\int_0^\infty\exp[i(\omega-k\omega_0-\omega_{21})t+g_s(t)]dt \end{aligned}$$

where $g_s(t)$ is given by Eq.(42) of the Appendix. Integrating with respect to t, one gets

$$\begin{aligned} W_a(\omega) &= \frac{\tau_s}{\pi}\exp(-S_0\coth\theta_0)\sum_{k=-\infty}^{\infty}I_k(\frac{S_0}{\sinh\theta_0}) \\ &\quad\times\exp(k\theta_0)\frac{\Phi(1,1+x_{ak};\sigma_{2s}\tau_s^2)}{x_{ak}} \end{aligned} \quad (30)$$

where $x_{ak}=\tau_s/(2T_1)+\sigma_{2s}\tau_s^2+i\tau_s(\omega_{21}-\omega+k\omega_0)$. Eq.(30) is the extension of Eq.(27) to the presence of high frequency intramolecular vibrations. For $\theta_0 >> 1$ we obtain

$$W_a(\omega)=\frac{\tau_s}{\pi}\exp(-S_0)\sum_{k=0}^{\infty}\frac{S_0^k}{k!}\frac{\Phi(1,1+x_{ak};\sigma_{2s}\tau_s^2)}{x_{ak}} \quad (31)$$

If the behavior of the wings of spectra is unimportant, one can use the "slow modulation" limit. In that case Eq.(31) may be replaced by

$$W_a(\omega)=\frac{\exp(-S_0)}{\sqrt{2\pi\sigma_{2s}}}\sum_{k=0}^{\infty}\frac{S_0^k}{k!}w(\frac{\omega-\omega_{21}-k\omega_0}{\sqrt{2\sigma_{2s}}}) \quad (32)$$

5.1 Explanation of introducing the empiric red shift of the absorption spectra of H-aggregates calculated in CES approximation

It is worthy to note that the CES approximation describes well the shape of the absorption spectra of H-aggregates. However, the spectra calculated in the CES approximation are blue shifted with respect to experimental ones.[33] To resolve the problem, the authors of Ref.[33] empirically introduced additional red shift that could be understood in the context of our more general theory as the red shift due to the CMLL mechanism. Indeed, let us write down Eq.(7) when both the self-energy ($\sim\tilde{\rho}_{21}$) and the population difference depends on the effective vibrational coordinate

$$\begin{aligned} &\frac{\partial}{\partial t}\tilde{\rho}_{21}(\alpha,t) \\ &\approx -i(\omega_{21}-\omega-p_1-\alpha)\tilde{\rho}_{21}(\alpha,t) \\ &\approx i[\frac{\mathbf{D}_{21}\cdot\mathbf{E}(t)}{2\hbar}+p_2\int\tilde{\rho}_{21}(\alpha,t)\,d\alpha]\rho_{11}^{(0)}(\alpha) \end{aligned} \quad (33)$$

Using the procedure described in Ref.,[17] we get an equation similar to Eq. (23) (together with Eq.(24)) with the only difference that ω_{21} should be replaced by $\omega_{21}-p_1$, and p - by p_2

$$\begin{aligned} \frac{\partial\rho_{11}(\alpha,t)}{\partial t} &= L_{11}\rho_{11}(\alpha,t) - \\ &\quad -\frac{\frac{\pi}{2}\rho_{11}^{(0)}(\alpha)|\Omega_R(t)|^2\delta(\omega_{21}-\omega-p_1-\alpha)}{|1+p_2\int d\alpha\rho_{11}^{(0)}(\alpha)\zeta(\omega+p_1-\omega_{21}+\alpha)|^2} \end{aligned} \quad (34)$$

Then similar to Eq.(25), we obtain

$$\frac{dn_1}{dt}=-\sigma_a(\omega_{21})\tilde{J}(t)\,\mathrm{Re}\,\frac{\bar{W}_a(\omega+p_1)}{1-ip_2\pi W_a(\omega+p_1)}+\frac{n_2}{T_1} \quad (35)$$

where the term $\mathrm{Re}\{\bar{W}_a(\omega+p_1)/[1-ip_2\pi W_a(\omega+p_1)]\}$ describes the absorption spectrum of molecules susceptible to the dipole-dipole intermolecular interactions expressed through their monomer spectra $W_a(\omega+p_1)$, Eqs.(30), (31) and (32).

Fig.4 shows the calculation results of the absorption spectrum of an H-aggregate according to the expression $\mathrm{Re}\{W_a(\omega+p_1)/[1-ip_2\pi W_a(\omega+p_1)]\}$ on the right-hand side of Eq.(35) and Eq.(31) (solid line), and its comparison with the monomer spectrum $\mathrm{Re}\,W_a(\omega)$ (dash line) and the spectrum of H-aggregate, $\mathrm{Re}\{W_a(\omega)/[1-ip_2\pi W_a(\omega)]\}$, calculated without the contribution of the CMLL mechanism (dash dot line). The values of parameters are found by fitting the experimental spectrum of the linear absorption of LD690 in methanol:[19] $\tau_s=10^{-13}s$, $k_BT=210\ cm^{-1}$, $\hbar\omega_{st}/(2k_BT)=1.99$, $S_0=0.454$,

Figure 4: Absorption spectra (in terms of τ_s/π) of the H-aggregate (solid line), the corresponding monomer (dash line) and the H-aggregate without the contribution of the CMLL mechanism (dash dot line) for $p_1 = 500\ cm^{-1}$ and $p_2 = -1500\ cm^{-1}$ Dimensionless parameter is $\Delta = \tau_s(\omega_{21} - \omega)$.

$\omega_0 = 1130\ cm^{-1}$, $\sigma_{2s} = \omega_{st} k_B T/\hbar$. The spectra presented in Fig.4 manifest that though the shape of the H-aggregate spectrum is fully described by the self-energy not depending on the effective vibrational coordinate, its position (including the additional red shift of the experimental spectra of H-aggregates[33]) may be correctly described only taking the CMLL mechanism into account. In other words, our more general theory enables us to describe both the shape and the position of the experimental spectra of H-aggregates due to the self-energy and the population difference ("lesser" GFs) both depending on the effective vibrational coordinate that leads to their frequency dependence. This can be understood as follows. The frequency dependent "lesser" GFs corresponding to the CES approximation describe well the spectral shapes of H-aggregates. The latters can interact with each other by the dipole-dipole interaction leading to the CMLL red shift that is described by the frequency dependent self-energy.

6 Bistability

We saw in Section5 that the dependence of both the self-energy and the population difference on vibrational coordinates manifests in experiment. Let us concentrate first on the self-energy depending on the effective vibrational coordinate. The corresponding Eqs. (8) and (14) for populations are nonlinear equations and can demonstrate a bistable behavior. We shall consider the CMLL mechanism of the dipole-dipole intermolecular interactions leading to the red shift (the first term on the right-hand side of Eq.(14)) when one can use Eqs.(16)-(17) for the monomer spectra. Fig.5 shows steady-state solutions of Eq.(14) for n_2 as a function of the power density of the exciting radiation $\tilde{J}$ at different detunings $\omega_{21} - \omega$. One can see that each value of $\tilde{J}$ within the corresponding interval produces three different solutions of Eq.(14) for dimensionless detunings $y = (\omega_{21} - \omega)/\sqrt{2\sigma_{2s}} = 0$, 0.25 and 0.5, however, only lower and upper branches are stable.[40] Such detunings correspond to the excitation at the short-wave part of the equilibrium absorption spectrum (see the Inset to Fig.5). As the excited state population increases, the spectrum exhibits the blue shift (see Eq.(14)) that should essentially contribute to the absorption. As a matter of fact, the bistable behavior of the population arises from the dependence of the resonance frequency of the molecules in dense medium on the number of excited molecules. In contrast, larger $y = 1$, 2.729 correspond to the excitation closer to the central part of the equilibrium absorption spectrum. In that case the blue shift produces lesser increasing the absorption and even can decrease it (for $y = 2.729$), so that the bistable behavior disappears.

6.1 Diminishing light intensity necessary for bistablity below the damage threshold

Since experiments on bistablity should be done with CW pumping or pulse pumping when the distance between pulses is smaller than the excited state lifetime T_1, the light intensity ought to be smaller than that in usual pulse experiments with thin films of dyes[15]

Figure 5: (Color online) Dependence of excited state population n_2 on power density of the exciting radiation $\tilde{J}$ at different detunings $\omega_{21}-\omega$. Dimensionless parameters are $J=\sigma_a\tilde{J}T_1$ and $y=(\omega_{21}-\omega)/\sqrt{2\sigma_{2s}}$. Parameters $\sqrt{\sigma_{2s}}$, ω_{st} and p are identical to those of Section4.1. Inset: Equilibrium spectra of the absorption (Abs) and the emission (Em); the arrows limit the frequency interval where calculated excited state populations n_2 show bistability.

Figure 6: 3-electronic states system. 1,2 - sinlet states, 3 - triplet state.

(as to CW pumping, the damage threshold should be much smaller than 1 MW/cm^2 [41]). The resolution of the problem may be achieved using 3-electronic states system with the long-living triplet state T_1 near (but below) the excited singlet state S_1, and fast intersystem crossing $S_1 \rightarrow T_1$, Fig.6. The rose bengal[42–45] and platinum-octaethyl-porphyrin (PtOEP)[46,47] are examples. They possess also large absorption cross-section ($\sigma_a \approx 10^{-15}$ cm^2 for PtOEP) that is necessary for significant light-induced change of the dielectric function. In such a case one can achieve strong depletion of the ground state S_0 using intensities much smaller than 1 MW/cm^2. Indeed, generalizing Eq.(14) to the three-level electronic system and bearing in mind Eqs.(16) and (17), one gets

$$\begin{aligned}\frac{dn_1}{dt} &= \sigma_a \exp[-\frac{(\omega_{21}-p\Delta n-\omega-\omega_{st})^2}{2\sigma_{2s}}]\tilde{J}\{n_2 - \\ &-n_1 \exp\left[\hbar\beta\left(\omega+p\Delta n-\omega_{21}+\frac{\omega_{st}}{2}\right)\right]\} \\ &+\frac{n_2}{T_1}+w_{31}n_3 \end{aligned} \quad (36)$$

Figure 7: Dependence of the ground state population n_1 on power density of the exciting radiation $\tilde{J}$ at dimensionless detuning $y = (\omega_{21} - \omega)/\sqrt{2\sigma_{2s}} = 0.5$ for $T_1 = 10^{-9}$ s. Probabilities of radiationless transitions, $w_{23} = 10^{10}$ s^{-1} and $w_{31} = 10^4$ s^{-1}, are close to those in rose bengal[42–45] and platinum-octaethylporphyrin (PtOEP).[46,47] Parameters $\sqrt{\sigma_{2s}}$, ω_{st} and p are identical to those of Section4.1.

$$\begin{aligned}\frac{dn_2}{dt} &= -\sigma_a \exp[-\frac{(\omega_{21} - p\Delta n - \omega - \omega_{st})^2}{2\sigma_{2s}}]\tilde{J}\{n_2 - \\ &-n_1 \exp\left[\hbar\beta\left(\omega + p\Delta n - \omega_{21} + \frac{\omega_{st}}{2}\right)\right]\} \\ &-n_2(\frac{1}{T_1} + w_{23}) \qquad (37)\end{aligned}$$

$$\frac{dn_3}{dt} = n_2 w_{23} - w_{31} n_3 \qquad (38)$$

where w_{ij} is the probability of radiationless transition $i \to j$, and $n_1 + n_2 + n_3 = 1$.

Fig.7 shows the steady-state solution of Eqs.(36), (37) and (38) for n_1 as a function of the power density of the exciting radiation $\tilde{J}$ for $y = (\omega_{21} - \omega)/\sqrt{2\sigma_{2s}} = 0.5$. One can see that the bistable behavior persists for the 3-electronic states system, however, involves much smaller light intensities than those for 2-electronic states system without triplet T_1 (see Fig.5). In addition, rose bengal is characterized by gigantic third order susceptibility $\chi^{(3)} \sim 10^{-3}$ esu.

7 Conclusion

In this work we have developed a mean-field theory of light-induced optical properties of photonic organic materials taking the collective effects into account. Our consideration is based on the model of the interaction of strong shaped laser pulse with organic molecules, Refs.,[17–19] extended to the dipole-dipole intermolecular interactions in the condensed matter. We show that such a generalization can describe both a red shift of the resonance frequency of isolated molecules, according to the CMLL mechanism,[20] and the wide variations of their spectra related to the aggregation of molecules into J- or H-aggregates. In particular case of weak radiation we recover the CES approximation.[32–34] We show that the experimental absorption spectra of H-aggregates may be correctly described only if one takes both mechanisms into account. Our theory contains experimentally measured quantities that makes it closely related to experiment.

The bistable response of organic materials in the condensed phase has been demonstrated using the electron-vibrational model. We have shown that using molecules with long-living triplet state T_1 near excited singlet state S_1, and fast intersystem crossing $S_1 \to T_1$ enables us to diminish CW light intensity needed for observing bistability below the damage threshold of thin organic films.

The phenomenon of bistability in spatially distributed systems can result in the generation of the switching waves in photonic organic materials.[16]

I thank M. A. Noginov for useful discussions and D. Huppert who attracted my attention to molecules Rose Bengal and platinum-octaethylporphyrin (PtOEP).

8 Appendix

In the case of the Gaussian modulation of the electronic transition by the vibrations, the absorption lineshape is given by[23,24,38,48]

$$F_a(\omega) = \frac{1}{\pi}\,\mathrm{Re}\int_0^\infty \exp[i(\omega - \omega_{21})t + g(t)]dt \qquad (39)$$

where

$$g(t) = -\int_0^t dt'(t-t')K(t') \qquad (40)$$

is the logarithm of the characteristic function of the spectrum of single-photon absorption after substraction of a term which is linear with respect to t and determines the first moment of the spectrum, $K(t)$ is the correlation function. Then

$$W_a(\omega) = \frac{1}{\pi}\int_0^\infty \exp[i(\omega-\omega_{21})t + g(t)]dt \qquad (41)$$

For the exponential correlation function $K_s(t) = \sigma_{2s}\exp(-|t|/\tau_s)$, we get

$$g_s(t) = -\sigma_{2s}\tau_s^2[\exp(-t/\tau_s) + \frac{t}{\tau_s} - 1] \qquad (42)$$

that leads to Eq.(27) of section 4.1.

References

[1] Durach, M.; Rusina, A.; Klimov, V. I.; Stockman, M. I. Nanoplasmonic renormalization and enhancement of Coulomb interactions. *New J. of Phys.* **2008,** *10,* 105011.

[2] Halas, N. J.; Lal, S.; Chang, W.-S.; Link, S.; Nordlander, P. Plasmons in Strongly Coupled Metallic Nanostructures. *Chem. Rev.* **2011,** *111,* 3913–3961.

[3] Maier, S. A. *Plasmonics: Fundamentals and Applications;* Springer: New York, 2007.

[4] Leonhardt, U.; Philbin, T. *Geometry and Light. The Science of Invisibility;* Dover Publications: Mineola, New York, 2010.

[5] Khurgin, J. B. How to deal with the loss in plasmonics and metamaterials. *Nature Nanotechnology* **2015,** *10,* 2–6.

[6] Hoffman, A. J.; Alexeev, L.; Howard, S. S.; Franz, K. J.; Wasserman, D.; Podolskiy, V. A.; Narimanov, E. E.; Sivco, D. L.; Gmachl, C. Negative refraction in semiconductor metamaterials. *Nature Materials* **2007,** *6,* 946–950.

[7] Koppens, F. H. L.; Chang, D. E.; de Abajo, F. J. G. Graphene Plasmonics: A Platform for Strong Light-Matter Interaction. *Nano Letters* **2011,** *11,* 3370–3377.

[8] Chen, J.; Badioli, M.; Alonso-Gonzalez, P.; Thongrattanasiri, S.; Huth, F.; Osmond, J.; Spasenovic, M.; Centeno, A.; Pesquera, A.; Godignon, P.; Elorza, A. Z.; Camara, N.; de Abajo, F. J. G.; Hillenbrand, R.; Koppens, F. H. L. Optical nano-imaging of gate-tunable graphene plasmons. *Nature* **2012,** *487,* 77–81.

[9] Fei, Z.; Rodin, A. S.; Andreev, G. O.; Bao, W.; McLeod, A. S.; Wagner, M.; Zhang, L. M.; Zhao, Z.; Thiemens, M.; Dominguez, G.; Fogler, M. M.; Neto, A. H. C.; Lau, C. N.; Keilmann, F.; Basov, D. N. Gate-tuning of graphene plasmons revealed by infrared nano-imagine. *Nature* **2012,** *487,* 82–85.

[10] Gu, L.; Livenery, J.; Zhu, G.; Narimanov, E. E.; Noginov, M. A. Quest for organic plasmonics. *Applied Phys. Lett.* **2013,** *103,* 021104.

[11] Gentile, M. J.; Nunez-Sanchez, S.; Barnes, W. L. Optical Field-Enhancement and Subwavelength Field-Confinement Using Excitonic Nanostructures. *Nano Letters* **2014,** *14,* 2339–2344.

[12] Fainberg, B. D.; Li, G. Nonlinear organic plasmonics: Applications to optical control of Coulomb blocking in nanojunctions. *Applied Phys. Lett.* **2015,** *107,* 053302 [Erratum, v. 107, 109902 (2015)].

[13] Li, G.; Shishodia, M. S.; Fainberg, B. D.; Apter, B.; Oren, M.; Nitzan, A.; Ratner, M. Compensation of Coulomb blocking and energy transfer in the current voltage characteristic of molecular conduction junctions. *Nano Letters* **2012,** *12,* 2228–2232.

[14] White, A. J.; Fainberg, B. D.; Galperin, M. Collective Plasmon-Molecule Excitations in Nanojunctions: Quantum Consideration. *J. Phys. Chem. Lett.* **2012,** *3,* 2738–2743.

[15] Tumkur, T. U.; Kitur, J. K.; Gu, L.; Zhu, G.; Noginov, M. A. Gigantic Optical Nonlinearity: Laser-Induced Change of Dielectric Permittivity of the Order of Unity *ACS Photonics* **2015,** *2,* 622–627.

[16] Fainberg, B. D.; Rosanov, N. N.; Veretenov, N. A. Light-induced "plasmonic" properties of organic materials: Surface polaritons and switching waves in bistable organic thin films. *Applied Phys. Lett.* **2017,** *110,* 203301.

[17] Fainberg, B. D. Nonperturbative analytic approach to interaction of intense ultrashort chirped pulses with molecules in solution: Picture of "moving" potentials. *J. Chem. Phys.* **1998,** *109,* 4523–4532.

[18] Fainberg, B. D.; Narbaev, V. Chirped pulse excitation in condensed phase involving intramolecular modes studied by double-sided Feynman diagrams for fast electronic dephasing. *J. Chem. Phys.* **2000,** *113,* 8113–8124.

[19] Fainberg, B. D.; Narbaev, V. Chirped pulse excitation in condensed phase involving intramolecular modes. II. Absorption spectrum. *J. Chem. Phys.* **2002,** *116,* 4530–4541.

[20] Klein, M. V.; Furtak, T. E. *Optics;* Willey: New York, 1988.

[21] Malyshev, V. A.; Moreno, P. Mirrorless optical bistability of linear molecular aggregates. *Phys. Rev. A* **1996,** *53,* 416–423.

[22] Glaeske, H.; Malyshev, V. A.; Feller, K. H. Effects of higher exciton manifolds and exciton-exciton annihilation on optical bistable response of an ultrathin glassy film comprised of oriented linear Frenkel chains. *Phys. Rev. A* **2002,** *65,* 033821(10).

[23] Fainberg, B. D. Ultrafast dynamics and non-Markovian processes in four-photon spectroscopy. In *Advances in Multiphoton Processes and Spectroscopy*, Vol. 15; Lin, S. H.; Villaeys, A. A.; Fujimura, Y., Eds.; World Scientific: Singapore, New Jersey, London, 2003.

[24] Mukamel, S. *Principles of Nonlinear Optical Spectroscopy;* Oxford University Press: New York, 1995.

[25] Fainberg, B. D. Theory of the non-stationary spectroscopy of ultrafast vibronic relaxations in molecular systems on the basis of degenerate four-wave mixing. *Opt. Spectrosc.* **1990,** *68,* 305 [Opt. Spektrosk., vol. 68, 525, 1990].

[26] Fainberg, B. Learning about non-Markovian effects by degenerate four-wave-mixing processes. *Phys. Rev. A* **1993,** *48,* 849.

[27] Fainberg, B. D. Non-linear polarization and spectroscopy of vibronic transitions in the field of intensive ultrashort pulses. *Chem. Phys.* **1990,** *148,* 33–45.

[28] Davydov, A. S. *Theory of Molecular Excitons;* Plenum: New York, 1971.

[29] Fainberg, B. D.; Levinsky, B. Stimulated Raman Adiabatic Passage in a Dense Medium. *Adv. Phys. Chem.* **2010,** *2010,* 798419.

[30] Crenshow, M. E.; Scalora, M.; Bowden, C. M. Ultrafast intrinsic optical switching in dense medium of two-level atoms. *Phys. Rev. Lett.* **1992,** *68,* 911–914.

[31] Abramowitz, M.; Stegun, I. *Handbook on Mathematical Functions;* Dover: New York, 1964.

[32] Eisfeld, A.; Briggs, J. S. The J-band of organic dyes: lineshape and coherence length. *Chem. Phys.* **2002,** *281,* 61–70.

[33] Eisfeld, A.; Briggs, J. S. The J- and H-bands of organic dye aggregates. *Chem. Phys.* **2006,** *324,* 376–384.

[34] Eisfeld, A.; Briggs, J. S. Absorption Spectra of Quantum Aggregates Interacting via Long-Range Forces. *Phys. Rev. Lett.* **2006,** *96,* 113003.

[35] Baker, Jr., G. A.; Graves-Morris, P. *Padé Approximants;* Addison-Wesley Publishing Company: London, 1981.

[36] Saibatalov, R. K.; Fainberg, B. D. Pade approximation for electronic-vibrational spectra and distribution functions of molecular systems with multiwell potentials. *Khim. Fizika (Chemical Physics)* **1987,** *6,* 163–169 [in Russian].

[37] Rautian, S. G.; Sobel'man, I. I. THE EFFECT OF COLLISIONS ON THE DOPPLER BROADENING OF SPECTRAL LINES. *SOVIET PHYSICS USPEKHI* **1967,** *9,* 701–716 [Usp. Fiz. Nauk 90, 209-238 (1966)].

[38] Fainberg, B. D. Stochastic theory of the spectroscopy of optical transitions based on four-photon resonance interaction and photo-echo-type effects. *Opt. Spectrosc.* **1985,** *58,* 323 [Opt. Spektrosk. v. 58, 533 (1985)].

[39] Lin, S. H. Spectral band shape of absorption and emission of molecules in dense media. *Theor. Chim. Acta* **1968,** *10,* 301.

[40] Bogoliubov, N. N.; Mitropolskyi, Y. A. *Asymptotic methods in the theory of non-linear oscillations;* Gordon and Breach: New York, 1961.

[41] Noginov, M. A. Private communication.

[42] Chang, C.-C.; Yang, Y.-T.; Yang, J.-C.; Wu, H.-D.; Tsai, T. Absorption and emission spectral shifts of rose bengal associated with DMPC liposomes. *Dyes and Pigments* **2008,** *79,* 170–175.

[43] Neckers, D. C. Rose Bengal. *Journal of Photochemistry and Photobiology, A: Chemistry* **1989,** *47,* 1–29.

[44] Larkin, J. M.; Donaldson, W. R.; Foster, T. H.; Knox, R. S. Reverse intersystem crossing from a triplet state of rose bengal populated by sequential 532- +1064-nm laser excitation. *Chemical Physics* **1999,** *244,* 319–330.

[45] Fini, P.; Loseto, R.; Catucci, L.; Cosma, P.; Agostiano, A. Study on the aggregation and electrochemical properties of Rose Bengal in aqueous solution of cyclodextrins. *Bioelectrochemistry* **2007,** *70,* 44–49.

[46] Bansal, A. K.; Holzer, W.; Penzkofer, A.; Tsuboi, T. Absorption and emission spectroscopic characterization of platinum-octaethylporphyrin (PtOEP). *Chemical Physics* **2006,** *330,* 118–129.

[47] Nifiatis, F.; Su, W.; Haley, J. E.; Slagle, J. E.; Cooper, T. M. Comparison of the Photophysical Properties of a Planar, PtOEP, and a Nonplanar, PtOETPP, Porphyrin in Solution and Doped Films. *J. Phys. Chem. A* **2011,** *115,* 13764–13772.

[48] Kubo, R. A Stochastic Theory of Line-Shape and Relaxation, In *Fluctuation and Resonance in Magnetic Systems*; ter Haar, D., Ed.; Oliver Boyd: Edinburgh, 1962.

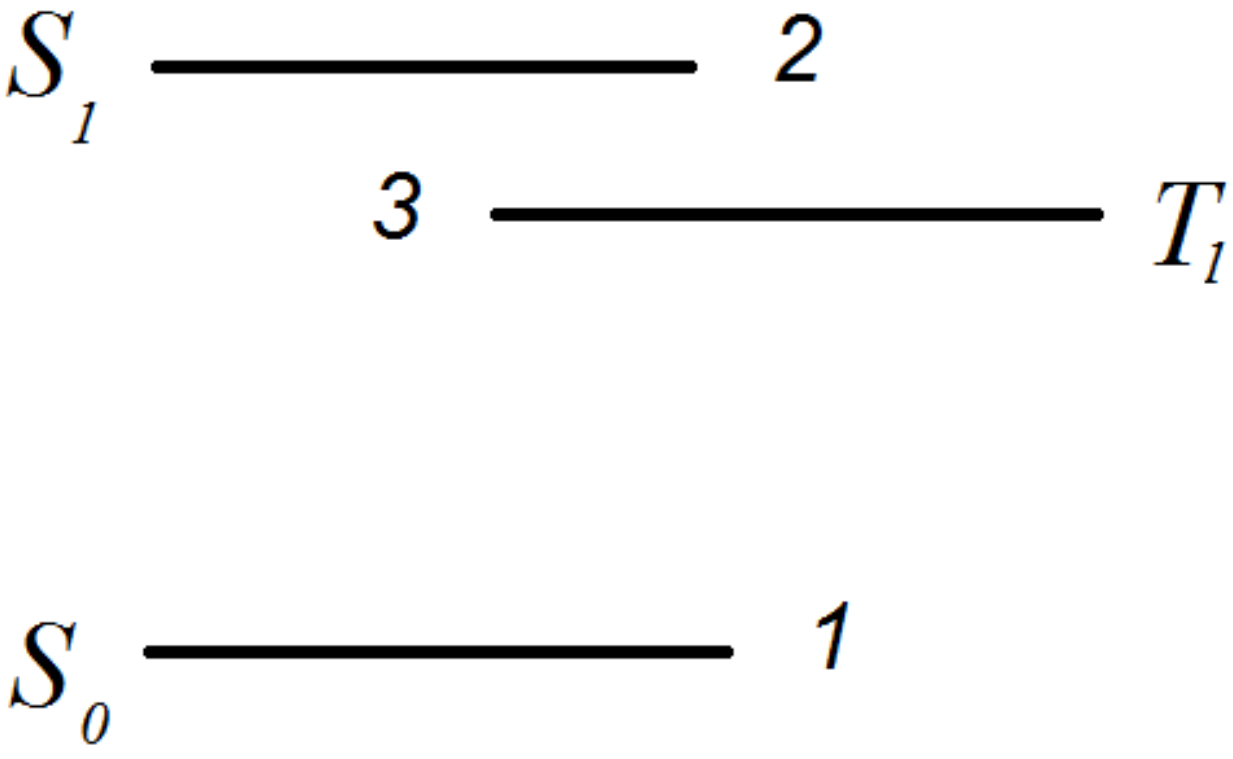

Figure 6

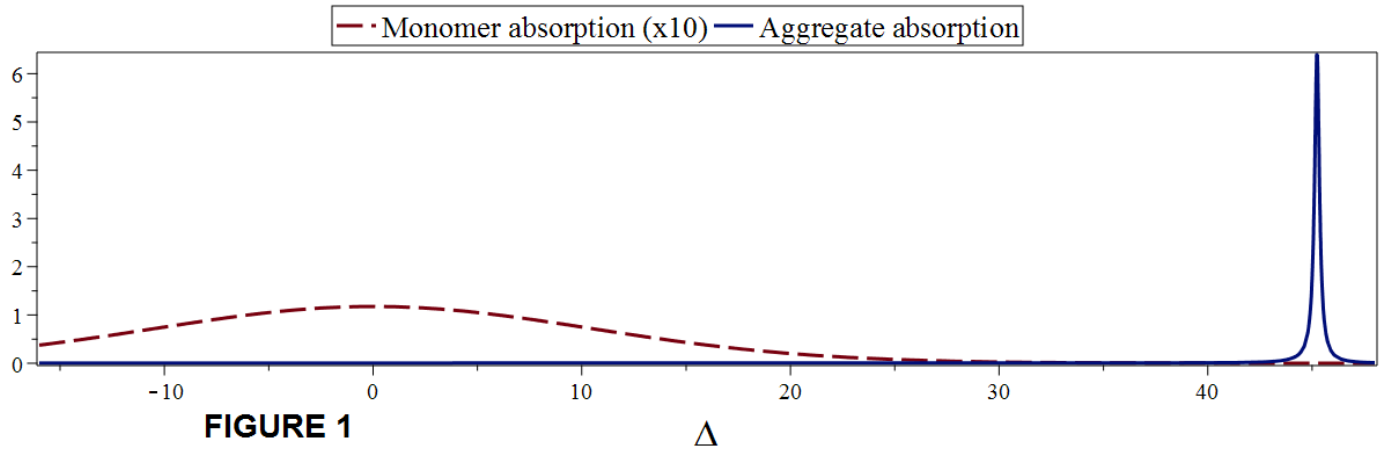
Monomer absorption (x10)
Aggregate absorption
6
5
4
3
2
1
0
-10
0
10
20
30
40
Δ

FIGURE 1

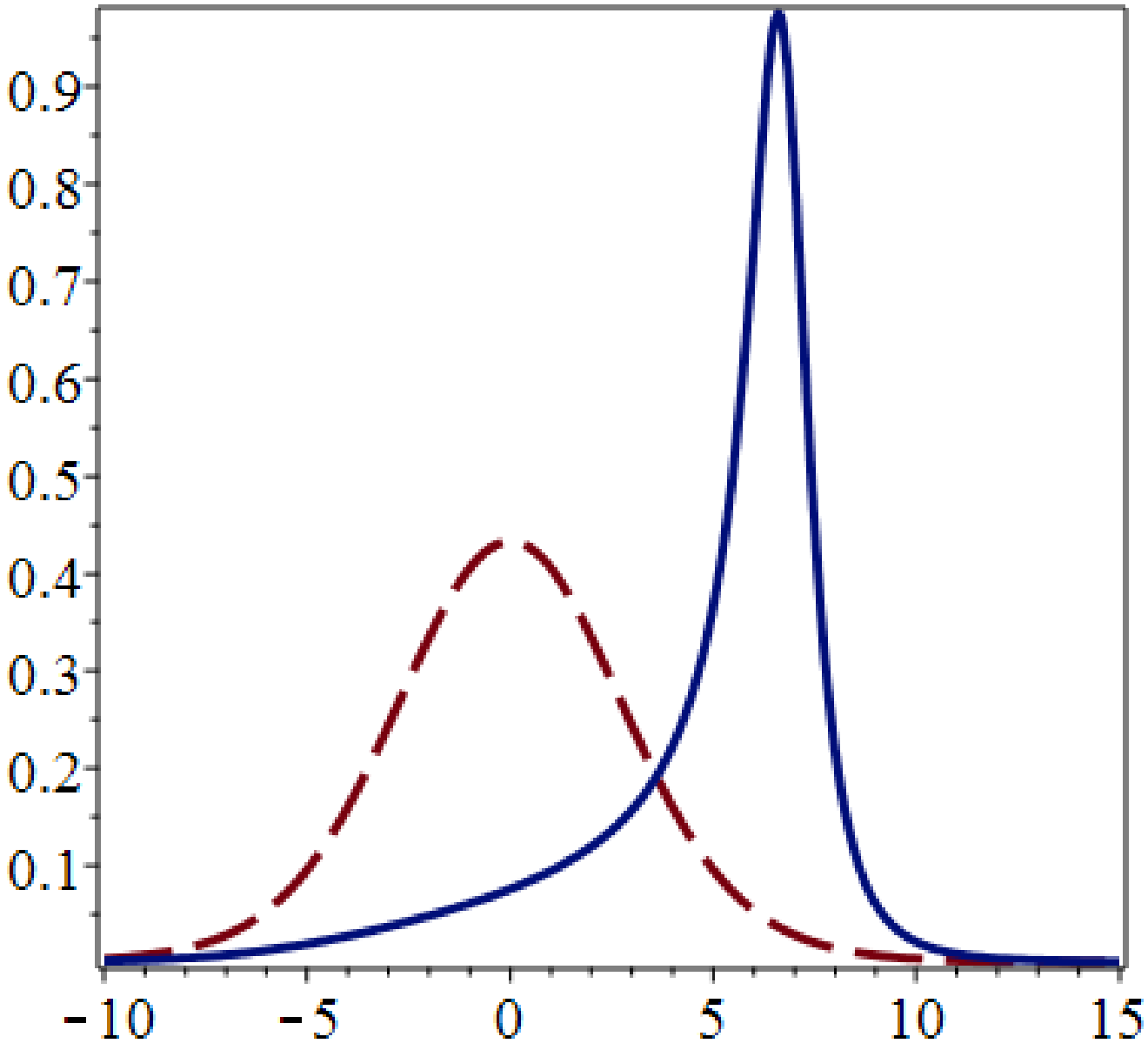

Figure 2

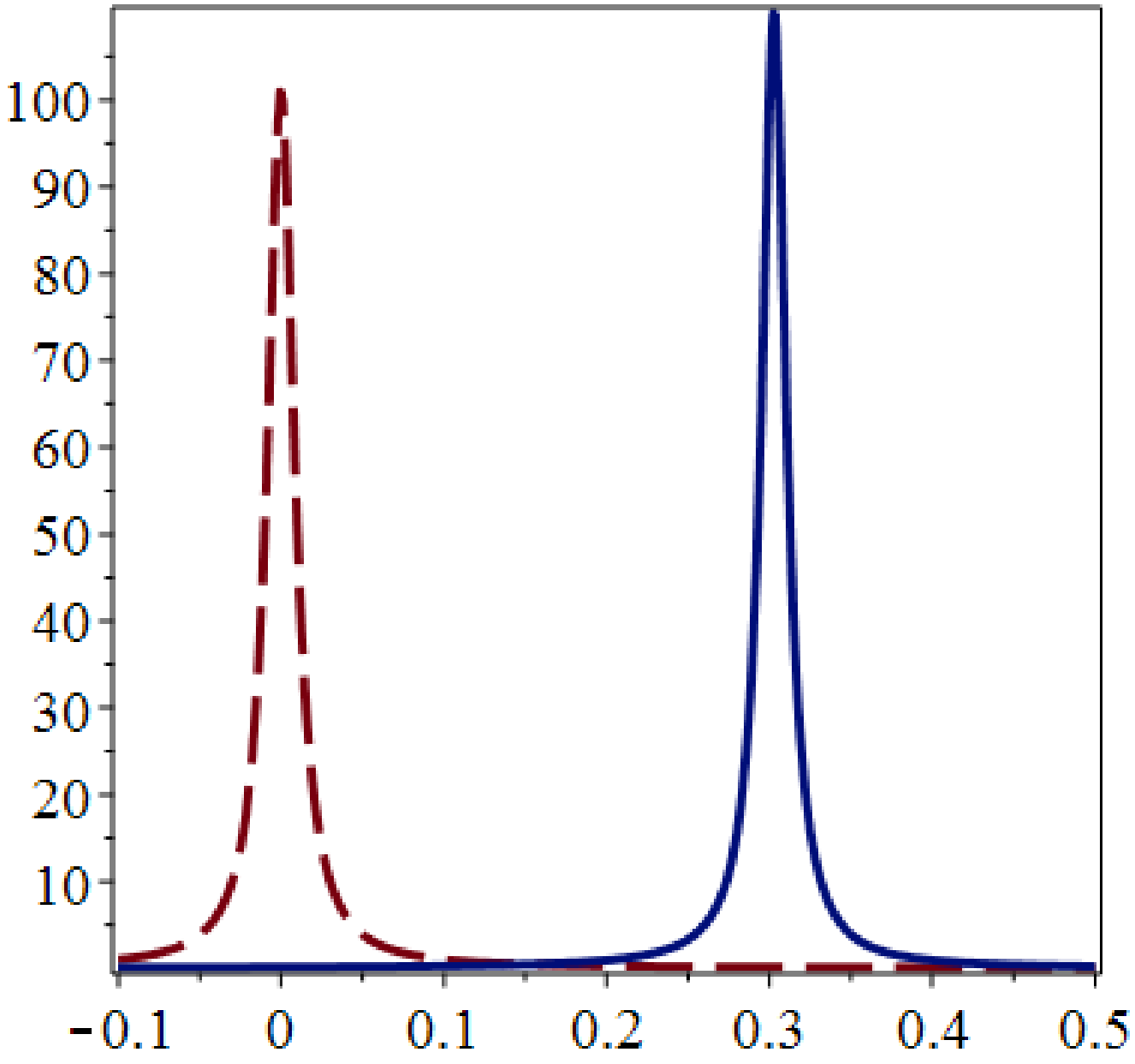

Figure 3

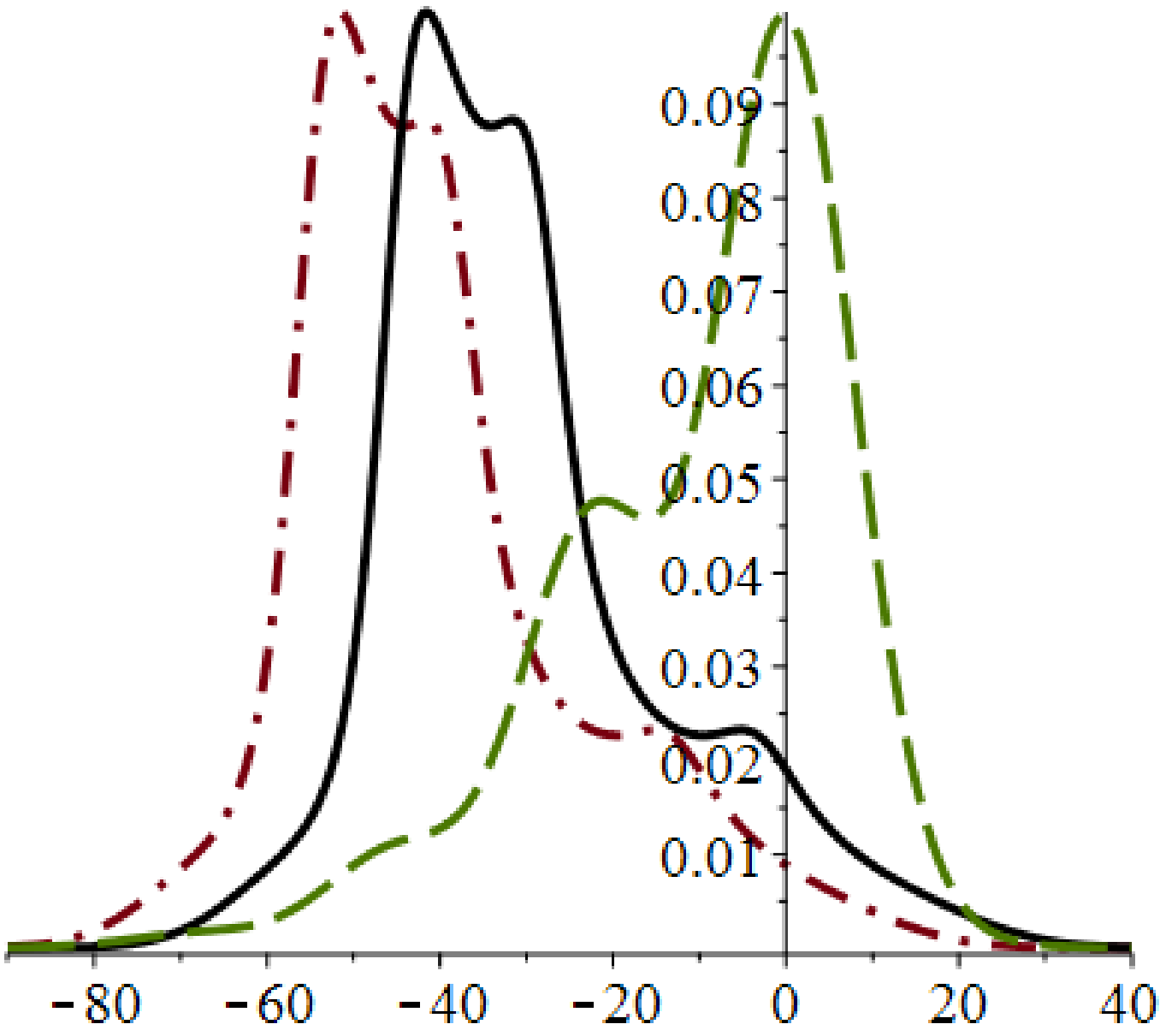

Figure 4

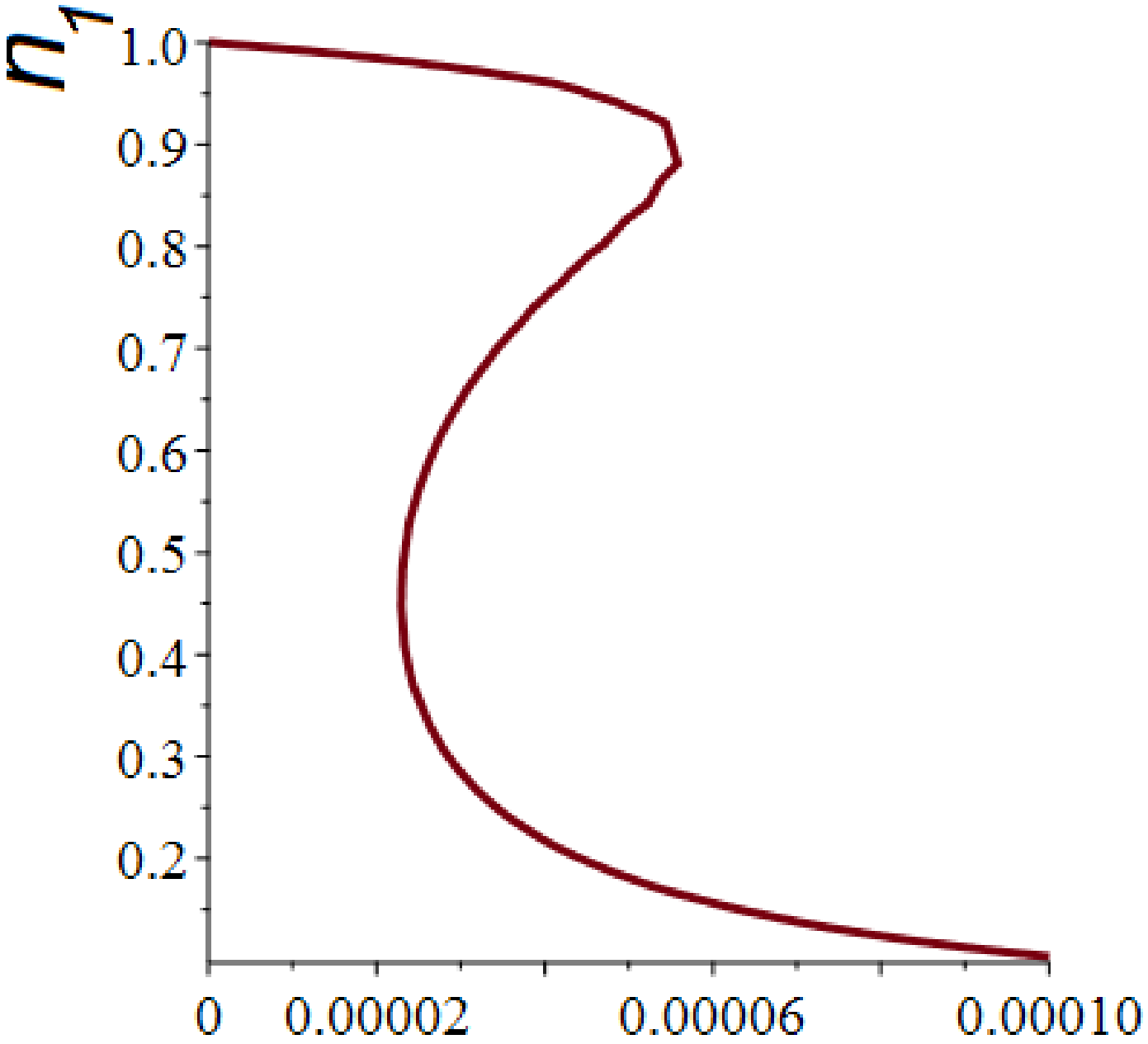

Figure 7

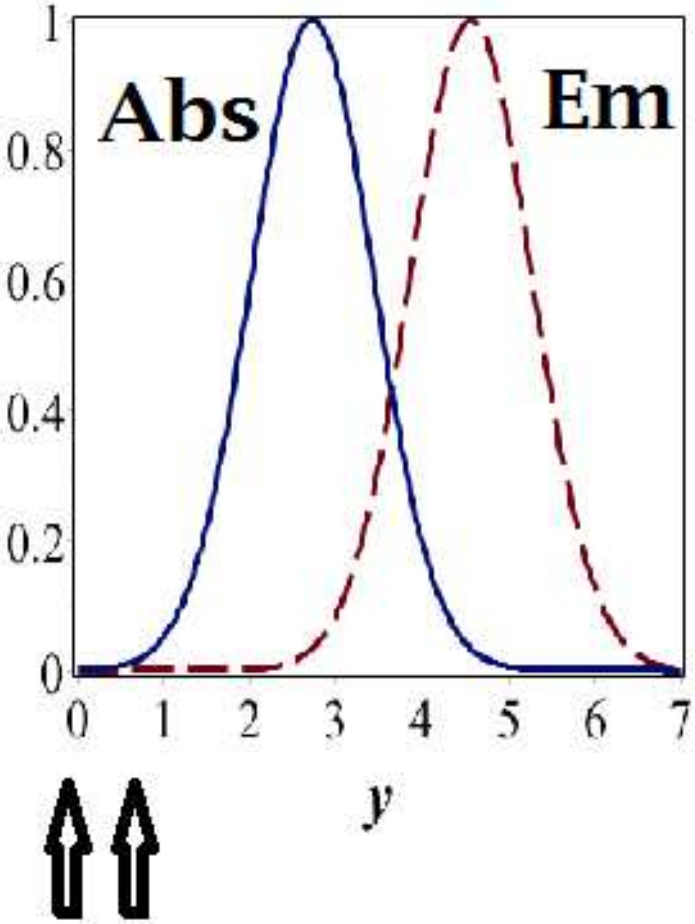
Abs
Em
1
0.8
0.6
0.4
0.2
0
0 1 2 3 4 5 6 7
y

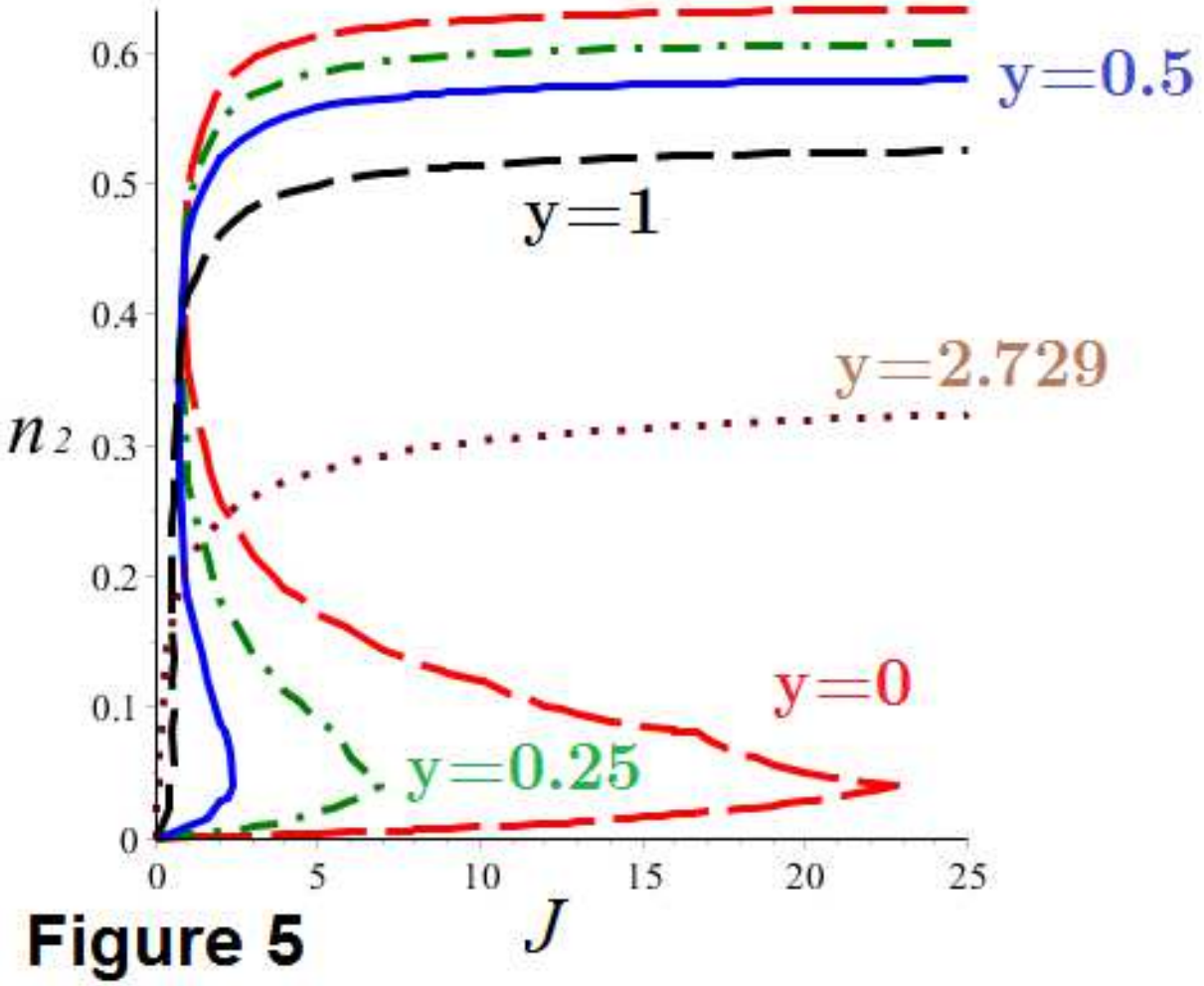
y=0.5
y=1
y=2.729
y=0
y=0.25
n2
0.6
0.5
0.4
0.3
0.2
0.1
0
0 5 10 15 20 25
J

Figure 5